Contents lists available http://www.kinnaird.edu.pk/

Journal of Natural and Applied Sciences Pakistan

Journal homepage: http://jnasp.kinnaird.edu.pk/

CHEMICAL CHARACTERIZATION, STRUCTURAL AND DIELECTRIC PROPERTIES OF NEWLY SYNTHESIZED MNXZN1-XFE2O4 NANOPARTICLES

Sajjad Ahmed[1], Uzma Ghazenfar*[1], Muhammad Nasir Akram[2], Javaid Riaz[3], Muhammad Shoaib[1], Anas Ramzan[1], Muhammad Rafi[1], Kashif Ghafoor[1]
[1]Department of Physics, University of Wah, 47040, Wah Cantt, Pakistan
[2]Center of Excellence in Solid State Physics, University of the Punjab, Lahore, Pakistan
[3]Department of Physics, University of Agriculture Faisalabad, Pakistan

Article Info

*Corresponding Authors
Email: khuzamajadoon@gmail.com

Abstract

Mn-Zn ferrite is a soft magnetic material used for electronic applications. These particles can be utilized for the application at the higher frequencies because of their excellent properties such as uniform and non-agglomerated. For achieving these properties, the Mn-Zn ferrite nanoparticles of chemical formula MnxZn1-xFe2O4 for x=0.1, 0.3, 0.5, 0.7, 0.9 were synthesized using the chemical co-precipitation technique. This chemical method was selected for the synthesis of nanoparticles due to its low cost, short reaction time, and the utilization of readily available chemicals. The sintering of samples was performed at 500oC for 5 hours and then grinded to make the fine powder. For structural and chemical phase analysis, Powder X-ray Diffraction and Fourier Transform Infrared Spectroscopy were employed (FTIR). The XRD pattern also ensured the production of cubic spinal structure; The 7600 plus Precision LCR meter was used to measure the dielectric properties of samples in pellet form (1.5mm thickness & 12mm diameter) in frequency ranging from 1kHz to 2MHz, at room temperature. The dielectric constant (real and imaginary parts) and tangent loss decreased when frequency indicated that normal dielectric behavior increased. The AC conductivity of ferrite samples increased with increased in frequency. This study, helpful will be helpful in the reduction of cost and the electronic devices to be sold will be cheap.

Keywords
Zn-Ferrite Nanoparticles, X-Ray Diffraction, Dielectric Nature, Co-Precipitation Technique

1. Introduction

Ferrites are the magnetic ceramics which are commonly used in the production of electronic components (Sadeghieh, 2017). Mn–Zn ferrites represents the important class of soft-ferrites materials that can synthesized through wet chemical methods such as the co-precipitation, hydrothermal synthesis, micro-emulsion synthesis x, and sol gel method (Narayankar *et al.*, 2012). In addition, various dry methods, including grinding (Sweetly & Joseph, 2007), mechanical alloying also used for synthesis of Mn–Zn ferrites (Waldron, 1955).

Mn–Zn ferrites can be diffused into myriad sizes and shapes for a variety of uses, and used primarily in the electronics field, power applications (Koops, 1951). These nanoparticles posees and electromagnetic interference (EMI) suppression (Sankpal, 1998). Potential application of Mn–Zn ferrites in electronic circuits continue to grow, with a variety of possible geometries, ever-improving material properties, and relative cost-effectiveness that makes ferrite components a traditional and innovative choice(Rao, 1981). They are generally used in transformer cores for electromagnets, capacitors in switch computers, and RF inductors with cubic spinel structures such as Manganese zinc ferrite Lithium ferrite, Nickel ferrite (Murugan, 2015). To the best of our knowledge, there is relatively less of work to describe the magnetic, electrical and dielectric properties of this important class of MnxZn1-xFe2O4 nanoferrites (Mansingh,1983).

In this study, we report the synthesis of MnxZn1-xFe2O4 nanoferrites nanoparticles by using co-precipitation process involving less energy and low-cost metal which is very easy to control on the required parameters which can result in good and well-organized ferrites. By controlling size of required particle in the range of nanometer (by the changing of synthesis condition like pH, and temperature) can gives lot of better results properties. We think that all the synthesis conditions at hand here will result in tuned values of electrical and dielectric properties of this material. Besides, to the best of our knowledge, most reports lack detailed calculations of the DC electrical resistivity; and also, different analytic techniques have been employed to study the structural, electrical, dielectric, and magnetic properties.

2. Materials and Methods

2.1. Sample Preparation

For the preparation of MnZnFe2O4 particles from metals, different chemicals and salts were used such as iron (III) chloride 6 hydrate (FeCl2 6H2O) manganese (II) chloride tetra hydrate (MnCl2.4H2O) and zinc chloride (ZnCl2) of Sigma company local distributer of chemicals. The purity of salts iron chloride was 99.9%, manganese chloride 99% and zinc chloride 99.5%. Sodium hydroxide (NaOH) base which was used as precipitating agent during the mixing of all chloride (Wang *et al.*, 2016).

2.2 Synthesis of Mnxzn1-Xfe2o4 Nanoferrites

The preparation of MnZnFe2O4for practical application doping of Mn in the following composition MnxZn1-xFe2O4 where x= 0 .1, x=0.3, x=0.5, x=0.7, x=0.9. These five samples were prepared by changing the X from 0.1 to 0.9 by chemical co precipitation method and label S1 for x=0.1, S2 for x=0.3, S3 for x=0.5, S4 for x=0.7, S5 for x=0.9 respectively (Rezai *et al.*, 2017).

2.3 Calculation

The accurate weight of each salt was mixed for preparation of every sample and calculated by the following formula, the molar mass of required salts is shown in Table1.

Moles = (required mass / molar mass of every salt)

Table 1: Shows the weight of chemical used in this study

Sr.no	**Salts name**	**Weight in gram/mole**	**Sr.no**
1	Zn Cl_2	169.02	1
2	Fe Cl_2	162.20	2
3	Mn Cl_2	197.91	3

Required sample were made by changing the value of x by using above formula, the calculated weights are listed in table 2. The Wight of every chemical in required range was measured by using the microgram.

Table 2: Shows the sample concentration and weight used in this study

Chemical name	**S1 X= 0.1**	**S2 X=0.3**	**S3 X=0.5**	**S4 X=0.7**	**S5 X=0.9**
$MnCl_2$	0.791 g	2.374 2g	3.958 2g	5.541 4g	7.124 7g
$ZnCl_2$	6.08g	4.732 g	3.380 g	2.028 2g	0.676 g
$FeCl_2$	12.97 6g	12.97 6g	12.97 g	12.97 6g	12.97 6g

The concentration of FeCl2 remaining the same in every sample, only we were changed the concentration of MnCl2 and ZnCl2 by doping formula i.e MnClxZn1-x FeCl3. In every sample, the precipitating agent used was NaOH and one molar solution in 100ml of water of NaOH was prepared by using the following formula.

Molarity= (mass of solution in gram /molar mass of solvent) × (1/volume of solution in dc3)

By using above formula, 4gram of NAOH was used for making the one molar solution of NAOH in distilled and de ionize water. After that, ZnCl2 solution was mixed into the MnCl2 solution at the room temperature and then the resulting solution of both chemicals was mixed into the FeCl3 solution. This final solution of all three salts were placed in magnetic starrier at 60 rpm for 30 mints, Now the one molar solution of sodium hydroxide (NaOH) was made in 100ml of distilled water, this solution is also places in moderate stirling for mixing, dark grey precipitate was observed, then mixture of both solutions were placed in pre heated water at 800 c for 60 mint. Then the resulting solution of MnCl2, ZnCl2 and FeCl3 NAOH were placed at temperature over night, after a day the

precipitate were filtered by using centrifuge at 6000rpm and then washing several times with distilled water and ethanol until the pH become 9 (Sweetly & Joseph, 2007).

2.4 Powder Formation

The filtered solution was placed for 5 hours in oven at 1000 c, the resulting formation was powder, then using the electric grander grand the final formation completely in powder form placed that powder in crucible and tag them (Farahani, 2013).

2.5 Heat Treatment

The tag crucible containing the fine powder was placed at 5000 c in furnace for 5 hours to ionize the gasses and other impurities. After 5 hours, the temperature of furnace to became at room temperature. After the heat treatment again using electric grander, grand the heated powder until it became the fine powder (Ali, 2011).

2.6 Pellet Formation

For making pellets, hydraulic press was used, dies were commonly made of steel, these dies make the circular pellets of varying diameter. Depends on material used, in the present work hard steel die were used for making the 12mm diameter and 1.5 mm width under the 120Mpa pressure(Hankare, 2011).

2.7 Characterization Techniques

X-ray diffraction techniques were used to check ferrite sample with compositions MnxZn1-xFe2 O4 for (x= 0.1,0.3, 0.5,0.7.0.9) by co precipitation method under homogenous powder was prepared of different concentration of Mn and zinc according to concentration formula given above is labeled as S1, S2, S3, S4 S5, were quenched the X -Ray diffraction pattern are took out by consuming Rigaku XRDD D/MAX-11A diffract meter using Cukα radiation and analyzed to calculate the inter atomic spacing "d" and miler index (h,k,l) (Zhang, 2009). By using Bragg's law

$$n\lambda=2d\sin\theta \quad \ldots\ldots(1)$$

Where θ=brag's angle

d= inter atomic spacing

hkl are miler plane index

XRD measurement were carried out the using radiation Cukα to confirm the chemical reaction completion and to identify the phase formed the and the sample were rotated through the angle of 200 to 800 with step size of 0.020 and scanning speed of 3×10-4 rad/sec, taken data from xrd machine were plotted, which were used to analyzed the inter planer distance and index (hkl) using JCPDS (joint committee on powder diffraction standard (Gillot, 1997).

3. Results and Discussion

All XRD patterns of materials were matched to those of the spinel MnZn ferrite (JCPDS No.74-2402) (Hilczer, 2014). Nearly no other crests were seen at the XRD arrangements. These outcomes for different sample with different Mn concentrations confirm the samples having altered PH values and different inhaling temperature prepared in whole some MnZn ferrite with spinel structures. In the samples size of the crystals, nano scaled which determine the

widening of peak in XRD pattern, with increase Ph, value in large crystal size that suggest by the narrower XRD (about 25 nm at pH of 12 and 17 nm at pH of 9) by co precipitation we can straight prepared the Nano particles of MnZn ferrite. The crystal size changes by changing the Ph value of solution. In our study, MnZnFe2O4 was prepared by varying the sintering temperature. Temperature of the water bath was kept at 60oc, 65oC, 70oc, 75oC and 80oC. Every sample was placed for 85 minutes in water bath. Spinel peak of sample 2 3 prepared at 65oC was more prominent then sample 5 which show the role of digestion temperature in spinal peaks. The characteristic peak was attained at an angle of 33.8, 33.3, 33.4, 33.3, 31.9, and degree 2θ with Cu Kα x-rays. The expansion of all the diffraction in XRD pattern designates the Nano-sized particle nature of the attained ferrites.

X-ray pattern of MnxZn1-xFe2O4 for x= 0.1, 0.3, 0.5, 0.7and 0.9 and peaks value data at table 3. the comparison of x-ray pattern shows a very small shift of XRD peaks of 2θ from 33.0308 to 33.3151 were observed corresponding to the reference peak (311) plane which confirms the replacement of Zn2+ ions by Mn2+ ions.

Table 3: Comparison of 311 planes of different compositions

Composition (x)	**Peak Height**	**Peak position (2θ)**	**$d_{(hkl)}$ A^0**	**Lattice parameter (a) A^0**
0.1	225	33.8	2.667	8.843
0.3	530	33.3	2.690	8.921
0.5	780	33.4	2.682	8.895
0.7	610	33.3	2.690	8.921
0.9	525	31.9	2.805	9.303

The lattice parameter can be calculated by using the fowling equation.

$$a = d\sqrt{h^2 + k^2 + l^2} \quad \text{……..(3)}$$

where,"d" is interplannar distance, "h k l" are Miller indices. "d" can be calculated using Bragg's equation as

$$2d \sin\theta = n\lambda \text{……..} \quad (4)$$

From lattice parameter values, it was seen that lattice parameter decreases for smaller Zn contents and vice versa with increase in Mn contents decrease in lattice parameter can be explain as the ionic radius of Mn2+ (0.91Ao) which is greater than ionic radius of Zn2+ (0.82Ao).

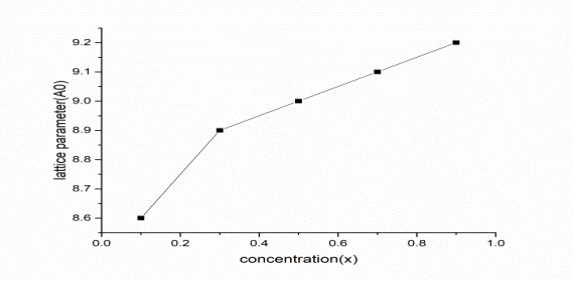

Figure 1: Shows the lattice parameter variation with composition

3.1 D-Spacing Variation

From table (3) it is cleared that with the increase of Mn concentration, the values of d-spacing

between lattices planes decreases. This can be described by concept that Mn ions produced lattice stress and strain which make reduction in d-spacing in the material.

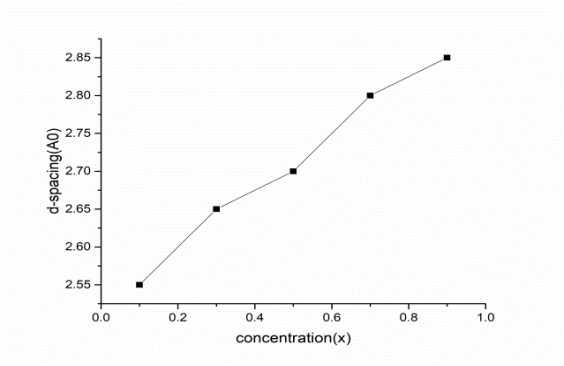

Figure 2: Shows the effect of Mn concentrations on d-spacing between lattices planes

3.2 Dielectric Parameters

Dielectric constant was measured by using the LCR Meter. For finding the dielectric properties, pelts of all samples were made with die of 12mm and width d 1.5mm and then coated with silver sheet which make the pellets good ohmic contacts with wires which are conducting. This can be defined 'the ratio of the charges that would be stored within the material defines as dielectric. Capacitance of the sample which is in the pellets form was determined by using the relation.

$\varepsilon' = C / C0$ …… (5)

C0 is the capacitance of free space

C is the capacitance of the material,

we use the relation for finding the C0

$C0 = \varepsilon 0 A/d$ …… (6)

Where ε0 is the permittivity of the free space and it has constant worth of (8.854×10-12 Fm-1).

$\varepsilon' = C d / \varepsilon 0 A$ …… (7)

The thickness of the pellet=d "A' is the cross-sectional area of the flat surface of the pellet made using the hydraulic press. When a dielectric material is open to the ac voltage, then these materials absorbed the electrical energy that is dissipated in the form of heat. This dissipation in the form of heat is called dielectric loss. When applied frequency matches with the relaxation time, then resonance occurs and gives the phase relationship between voltage and current. So, the current lead to voltage by (90-δ), where tan δ is the electrical loss due to resonance and called as tangent loss, δ is called the loss angle and the tangent loss can be expressed as:

$\text{Tan } \delta = \varepsilon'' / \varepsilon'$ …… (8)

As Dielectric constant is complex quantity so have real (ε') and imaginary (ε″) parts. The real part of dielectric ε' describes the storage while imaginary part of dielectric ε″ gives loss of energy during each cycle of the electric field applied. The dielectric constant (ε'), dielectric loss (ε″) were calculated by above formulas(Sindhu, 2002). Both real and imaginary parts of dielectric constant depend on frequency showing ferromagnetic behavior i.e., dielectric constant have large value at low frequency and when we increasing the range of

frequency, value of dielectric constant decreases. At low frequency, it shows the phenomenon of dispersion. For all samples with different doping of Mn, comparison of frequency dependent on dielectric constant (ε' and ε″) is shown in figure 3(A, B, C, D).

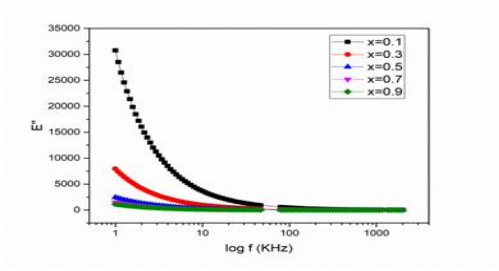

A

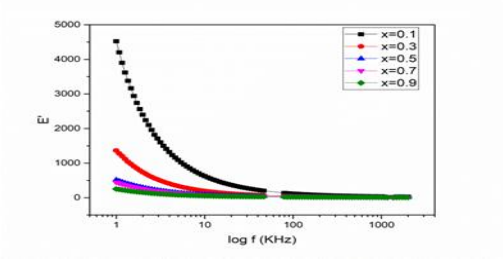

B

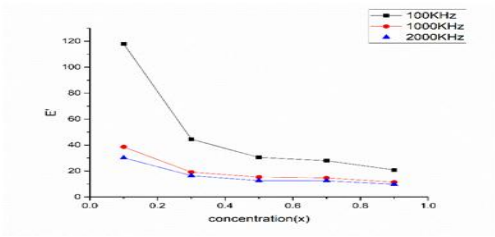

C

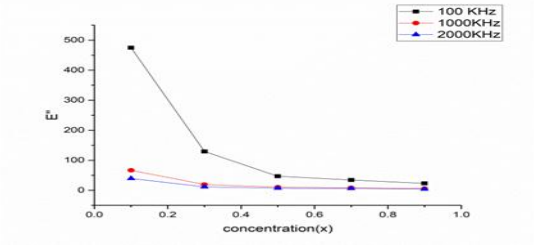

D

Figure 3: (A,B, C, D): Shows the different doping of Mn, comparison of frequency dependence on dielectric constant (ε' and ε″)

Dielectric constant at lower frequency shows the dispersion which shows that process of polarization as followed of Maxwell –Wagner interfacial polarization (Lakshman, 2005). According to this, model ferrites possess the highly conducting grains were separated by weakly conducting grain boundaries(El-Sayed, 2003). Ferrites become dipolar due to the presence of Fe2+ and Fe 3+ ions. The electron bounding between ferrous (Fe2+) and ferric (Fe3+) ions in the ferrite lattice reasons dielectric polarization. From above all result and discussion the dielectric constant is a joint effect of different polarizations including dipolar, electronic, ionic, and interfacial (Hankare, 2011). At lower frequency, dominant contribution to the dielectric constant by interfacial dipolar polarizations. When there is increase in frequency, polarization occurs due to orientation. Ionic sources decrease and finally become zero because of the lethargy of particles and ions. Dielectric constant remains unaffected in high frequency zone, which is effect of altercation of electrons amongst Fe2+ and Fe3+ in an n-type ferrite, Among Mn3+ and Mn2+ in a p-type ferrite exchange of hole cannot follow the frequency of alternating field applied after a critical value of the frequency (Zhang, 2009). For high frequency application materials having small dielectric constant are exactly appropriate.

The process of diffusion depends of the electromagnetic surfs, actual that the little value of dielectric continuous growths and this decreases skin effects (Nalbandian, 2008).

3.3 Variation In Tangent Loss With Frequency And Mn Concentration (X):

The dielectric tangent loss and energy loss are parallel dipoles domain wall motion by alternating electric field. Domain wall motion leads to cause the higher values of loss at lower frequencies range, because of which heat was dissipate in large amount (Mathew, 2007). But due to rotation at higher frequency, the domain wall motion constrains and the position of polarization changed by force. This rotation does not respond to change the position of polarization at higher frequency so, a very small amount of heat is dissipated (Solyman, 2006).

It is clear that with increasing frequency dielectric and tangent loss both decreases initially and then becomes saturated. The dissipation factor in saturation point is much clear and easily find, as compared to dielectric constant. The decrease or loss due to skin effect in dielectric constant which is function of frequency may be recognized to the detail that electronic conversation between captions which cannot track the frequency pattern resulting the Debye relaxation process (Shokrollahi, 2008). Number of features such as physically in similarity, Fe+2 contents, non-stoichiometric, etc. effect the dielectric tangent loss, which can be determined by preparation method with the help of Koop's model the relation between of dielectric loss and frequency can be explained (Dasgupta, 2006). The increase in Mn concentrations dielectric tangent loss decreases, indicating this fact that the bigger grain causes greater Df value. the Df variation with different Mn concentration at 2000 kHz, 1000 kHz and 100 kHz due to rearrangement of octahedral (B) tetrahedral (A) sites, making a mixed cationic distribution. Conductivity with respect to frequency and Mn concentration (x) as shown inn Fig-4(A, B).

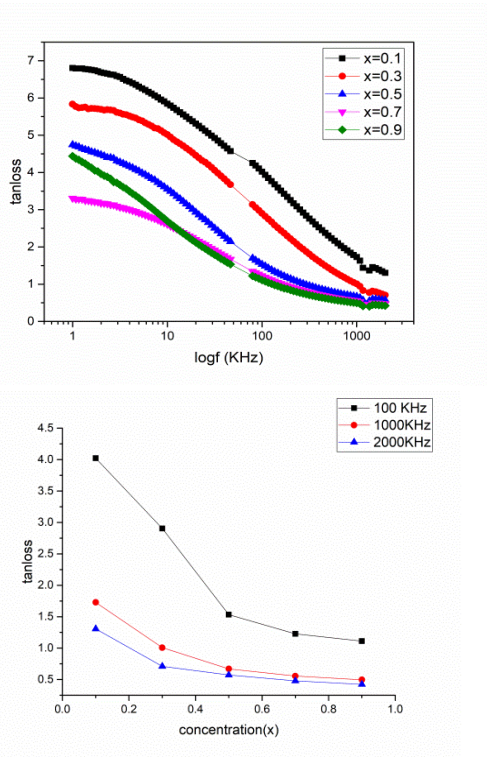

Figure 4: (A,B): Conductivity with respect to frequency and Mn concentration (x)

The AC conductivity of the samples were resulted from dielectric constant and Df using the equation [24]; Df=tangent loss

бac = ωεoε'tanδ……. (9)

also, we know that

ε” = ε’tanδ……. (10)

Ac conductivity can be calculated as;

бac = ωεoε” ……. (11)

ω = 2Πf……. (12)

Every samples with increasing frequency shows increase in AC conductivity and fallows the dynamical law [25]

σ(ω)=Aωs……. (13)

where ‘A’ is used for limit with the conductivity unit and ‘s’ is used for the slope of the linear plot of frequency depends upon conductivity. An increase in Mn concentrations causes the conductivity of the samples decreases.

The Mn ions shows the great partiality for the octahedral [B] sites, so by substituted it replaced Fe+3 ions. The probability of ions exchange between Fe+2 and Fe+3 reduces with the reduction of Fe+3 and results a significant decrease in Ac conductivity(Ullah, 2013). The Maxwell Wagner model also explains the Ac Conductivity according to which a thin layer of ill conducting grain boundary separated the well conducting grains. When size of grains increases, the construction the oxygen layer on the grain boundary is probable (Selvan, 2008).

In the conduction process, grains become greater magnitude donate more at high frequency due to the steady decrease in initiation energy barrier (shaped by grain boundaries) with frequency. In our case, AC conductivity also decreased due to grain magnitude of the sintered samples decreased. As Mn concentration increase which produce greater coulomb field in its locality and reduce Fe+3ions in octahedral sites which is responsible for electron hopping, viewing a lesser worth of conductivity shown in Figure the ac conductivity difference with different Mn concentration at 2000 kHz, 1000 kHz and 100 kHz(Nasir, 2011).. The increase (x=0.1-x=0.3) and then decrease (x=0.5 – x=0.9) in conductivity due to rearrangement of cat ions on tetrahedral (A) and octahedral (B) sites, starting a mixed cationic distribution. Ac conductivity with respect to frequency and Mn concentration (x) as shown in Fig-5(A, B).

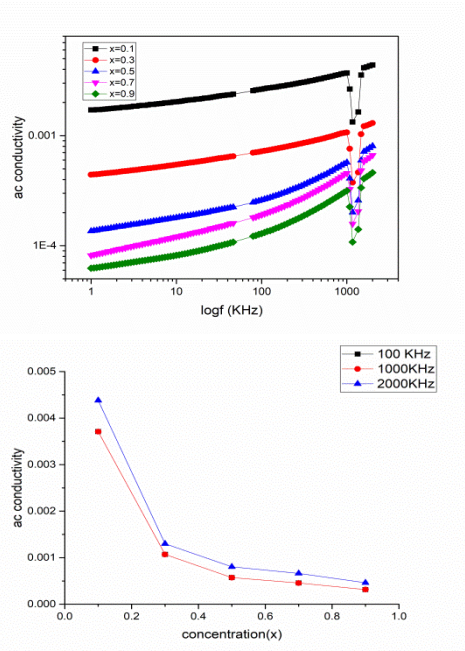

Figure 5: (A, B): ac conductivity with respect to frequency and Mn concentration (x)

The dielectric study carried out by 7600 plus Precision LCR meter in 1 kHz -2 MHz range revealed the normal dielectric behavior of ferrites. Dielectric constant (ε”), dielectric loss(ε"), and loss tangent (tan δ) decreased with frequency showing dispersion in low frequency

region and remained steady state in high frequency region(Hilczer, 2014). The AC conductivity (σ) of prepared samples showed increasing trend with frequency due to the 2 small losses at the high frequency. Dependence of all these parameters (ε'), ε", tan δ, σ) on Mn concentration was also checked. It decreased by increasing Mn contents (x). Maxwell-Wagner and Koop"s model was used to explain dielectric polarization and conduction mechanisms in Mn-Zn ferrites (Sharifi, 2012).

4. Conclusion

Mn-Zn ferrite (MnxZn1-xFe2O4, for x= 0.1, 0.3, 0.5, 0.7. 0.9) nanoparticles synthesized using chemical co-precipitation method. X-ray analysis explored that nanoparticle for each value of x had cubic spinal structure. No extra peaks were observed in XRD spectra indicating the absence of any un-reacted component in the samples. The d-spacing and lattice parameter were found to lie ranging from 2.54Ao to 2.51 Ao, and from 8.42Ao to 8.33Ao respectively. Both of them were decreased by increasing Mn doping. This trend is due to the fact that ionic radius of Mn2+ ions is greater than Zn2+ and also Mn2+ ions have stronger preference for octahedral sites. The crystallite size was observed to vary between 10-13nm and its value was maximum for x=0.3. This study will helpful for discovering the novel nanoparticles with low cost and maximum activity using them in electronics.

5. References

Ata-Allah, S. S., & Kaiser, M. (2004). Semiconductor- to- metallic transition in Cu- substituted Ni–Mn ferrite. physica status solidi (a), 201(14), 3157-3165.

Dasgupta, S., Kim, K. B., Ellrich, J., Eckert, J., & Manna, I. (2006). Mechano-chemical synthesis and characterization of microstructure and magnetic properties of nanocrystalline Mn1− xZnxFe2O4. Journal of alloys and compounds, 424(1-2), 13-20.

El-Sayed, A. M. (2003). Electrical conductivity of nickel–zinc and Cr substituted nickel–zinc ferrites. Materials Chemistry and Physics, 82(3), 583-587.

Gillot, B., & Domenichini, B. (1997). Effect of the preparation method and grinding time of some mixed valency ferrite spinels on their cationic distribution and thermal stability toward oxygen. Materials chemistry and physics, 47(2-3), 217-224.

Hankare, P. P., Patil, R. P., Sankpal, U. A., Jadhav, S. D., Garadkar, K. M., & Achary, S. N. (2011). Synthesis and morphological study of chromium substituted Zn–Mn ferrites nanostructures via sol–gel method. Journal of alloys and compounds, 509(2), 276-280.

Hilczer, A., Andrzejewski, B., Markiewicz, E., Kowalska, K., & Pietraszko, A. (2014). Effect of thermal treatment on magnetic and dielectric response of SrM hexaferrites obtained by hydrothermal synthesis. Phase Transitions, 87(10-11), 938-952.

Koops, C. G. (1951). On the dispersion of resistivity and dielectric constant of some semiconductors at audiofrequencies. Physical review, 83(1), 121.

Lakshman, A., Rao, P. S., Rao, B. P., & Rao, K. H. (2005). Electrical properties of In3+ and Cr3+ substituted magnesium–manganese ferrites. Journal of Physics D: Applied Physics, 38(5), 673.

Mansingh, A., & Dhawan, V. K. (1983). AC conductivity of V2O5-TeO2 glasses. Journal of Physics C: Solid State Physics, 16(9), 1675.

Mathew, D. S., & Juang, R. S. (2007). An overview of the structure and magnetism of spinel ferrite nanoparticles and their synthesis in microemulsions. Chemical engineering journal, 129(1-3), 51-65.

Nalbandian, L., Delimitis, A., Zaspalis, V. T., Deliyanni, E. A., Bakoyannakis, D. N., & Peleka, E. N. (2008). Hydrothermally prepared nanocrystalline Mn–Zn ferrites: synthesis and characterization. Microporous and Mesoporous Materials, 114(1-3), 465-473.

Nasir, S., & Anis-ur-Rehman, M. (2011). Structural, electrical and magnetic studies of nickel–zinc nanoferrites prepared by simplified sol–gel and co-precipitation methods. Physica Scripta, 84(2), 025603.

Nasir, S., & Anis-ur-Rehman, M. (2011). Structural, electrical and magnetic studies of nickel–zinc nanoferrites prepared by simplified sol–gel and co-precipitation methods. Physica Scripta, 84(2), 025603.

Rao, K. H., Raju, S. B., Aggarwal, K., & Mendiratta, R. G. (1981). Effect of Cr impurity on the dc resistivity of Mn- Zn ferrites. Journal of Applied Physics, 52(3), 1376-1379.

Sankpal, A. M., Suryavanshi, S. S., Kakatkar, S. V., Tengshe, G. G., Patil, R. S., Chaudhari, N. D., & Sawant, S. R. (1998). Magnetization studies on aluminium and chromium substituted Ni–Zn ferrites. Journal of magnetism and magnetic materials, 186(3), 349-356.

Selvan, R. K., Augustin, C. O., Šepelák, V., Berchmans, L. J., Sanjeeviraja, C., & Gedanken, A. (2008). Synthesis and characterization of CuFe2O4/CeO2 nanocomposites. Materials Chemistry and Physics, 112(2), 373-380.

Sharifi, I., Shokrollahi, H., & Amiri, S. (2012). Ferrite-based magnetic nanofluids used in hyperthermia applications. Journal of magnetism and magnetic materials, 324(6), 903-915.

Shokrollahi, H. (2008). Magnetic properties and densification of Manganese–Zinc soft ferrites (Mn1-xZnxFe2O4) doped with low melting point oxides. Journal of Magnetism and Magnetic Materials, 320(3-4), 463-474.

Shokrollahi, H., & Janghorban, K. (2007). Influence of additives on the magnetic properties, microstructure and densification of Mn–Zn soft ferrites. Materials Science and Engineering: B, 141(3), 91-107.

Sindhu, S., Anantharaman, M. R., Thampi, B. P., Malini, K. A., & Kurian, P. (2002). Evaluation of ac conductivity of rubber ferrite composites from dielectric measurements. Bulletin of Materials Science, 25(7), 599-607.

Solyman, S. (2006). Transport properties of La-doped Mn–Zn ferrite. Ceramics international, 32(7), 755-760.

Ullah, Z., Atiq, S., & Naseem, S. (2013). Influence of Pb doping on structural, electrical and magnetic properties of Sr-hexaferrites. Journal of Alloys and Compounds, 555, 263-267.

Waldron, R. D. (1955). Infrared spectra of ferrites. Physical review, 99(6), 1727.

Zhang, C. F., Zhong, X. C., Yu, H. Y., Liu, Z. W., & Zeng, D. C. (2009). Effects of cobalt doping on the microstructure and

magnetic properties of Mn–Zn ferrites prepared by the co-precipitation method. Physica B: Condensed Matter, 404(16), 2327-2331.